

# Design principles for aqueous interactive materials: Lessons from small molecules and stimuli responsive systems

Jade A. McCune<sup>†</sup>, Stefan Mommer<sup>†</sup>, Christopher C. Parkins<sup>†</sup> and Oren A. Scherman<sup>\*</sup>

## Abstract

Interactive materials are at the forefront of current materials research with few examples in the literature. Researchers have been inspired by nature to design and develop materials, which can modulate and adapt their behavior in accordance with their surroundings. The past decades have seen the development of stimuli-responsive systems which, although often described as smart, lack the ability to act autonomously and are typically static and free of influence from their environment. Nevertheless, these systems have attracted much attention on account of the resultant materials' ability to change their properties in a predictable manner with an applied stimulus. Thus, stimuli-responsive materials have found application in a plethora of areas including drug delivery, artificial muscles, camouflage systems etc. Stimuli-responsive materials are now serving as the precursors and basis for the design and realization of the next generation of interactive materials. The interest in these systems has resulted in a library of well developed chemical motifs however, there is a fundamental gap between stimuli-responsive and interactive materials. In this perspective, we aim to outline the current state-of-the-art stimuli-responsive materials with a specific emphasis on aqueous macroscopic interactive materials. Compartmentalization, critical for achieving interactivity, relies on hydrophobic, hydrophilic, supramolecular, ionic interactions, which are commonly present in aqueous systems and enable complex self-assembly processes. We outline the relevant examples of aqueous interactive materials that do exist and suggest design principles that should be followed to realize the next generation of materials with embedded autonomous function.

## Introduction

Nature is inherently interactive, sensing changes in the external environment and augmenting behavior accordingly. Such interactive behavior is especially prevalent in biological systems within nature, where autonomous response and

self-regulation are key to almost all processes that dictate life. Biological systems, such as cells, show extraordinary complexity and have the ability to carry out a plethora of advanced functions in response to external environmental changes.<sup>[1]</sup>

Synthetic electronic systems, designed and built to show interactive behavior, have been developed from small components such as logic gates up to larger systems such as computers. Driven to understand how to design and introduce interactivity into passive systems, humans began to build complex machines, computers that process commands and ultimately develop artificial intelligence.<sup>[2]</sup> Defining interactivity within a chemical system is more complex. One of the requirements to form an interactive material from chemical building blocks (Figure 1) is that the system must be able to respond selectively to external stimuli (or environmental changes) and adapt its behavior accordingly. Stimuli-responsive materials are able to detect a stimulus applied remotely (e.g. through heat, change in pH, magnetic field or light) and transform it into a chemical output.<sup>[3,4]</sup> They differ from interactive materials as they often have a one-way exchange of information, for example in a photoresponsive system an input  $S_1$  is introduced (light) and an output observed (e.g. cargo release, contraction of material, etc.) this is a one-way process, Equation 1.



In other cases, the processes can be reversible however, this relies on the introduction of a second stimuli ( $S_2$ ) which is different from the first ( $S_1$ ), Equation 2. This can be a different wavelength of light in the switching between *trans* and *cis* states of azobenzenes or heating and cooling in the case of thermoresponsive polymeric materials.<sup>[5,6]</sup>



Although these materials are often described as 'smart', they are far from being interactive as communication between different states does not exist. The current state-of-the-art stimuli responsive materials (Figure 1) are serving as the precursor to the next generation of interactive materials.

<sup>\*</sup> J. A. McCune, S. Mommer, C. C. Parkins and O. A. Scherman  
Melville Laboratory for Polymer Synthesis,  
Department of Chemistry, University of Cambridge  
Lensfield Road, Cambridge, CB2 1EW, UK  
E-mail: oas23@cam.ac.uk

<sup>†</sup> These authors contributed equally

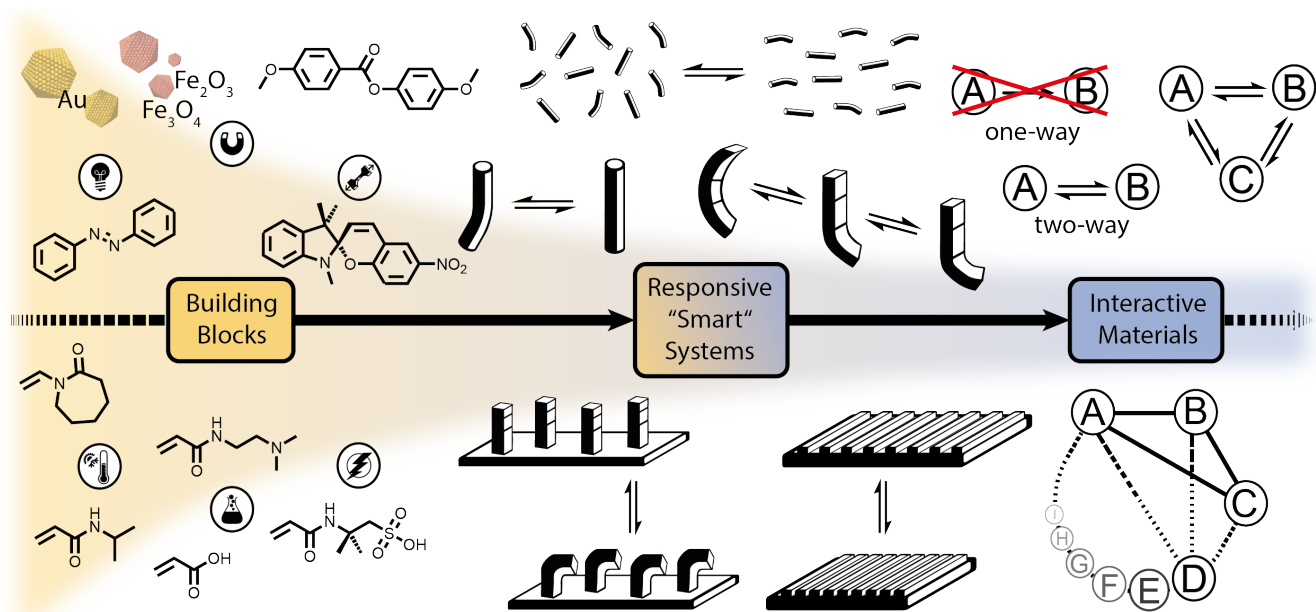


**Figure 1** Schematic representation of the development towards interactive supramolecular water-based materials. Responsive chemical building blocks have been designed and synthesised. These moieties were incorporated into “smart” materials to create responsive materials. Simple interactive materials are beginning to emerge, with more complex systems forthcoming.

The area is relatively new and there are many hurdles to overcome before aqueous interactive materials can flourish. Existing limitations include the limited scope of chemical moieties that can impart interactive behavior and their solubility in water. Isolation of different chemical states, preparation of materials with orthogonal behavior and the inefficient switching of chemical systems in equilibrium compared to nature are other important factors limiting the development of this area. To become truly interactive, all processes between states need to be reversible and involve exchange of information between a minimum of two states, Figure 1. Enhanced functionality of the interactive material can be achieved by increasing the number of states; however, with this comes a significant increase in complexity. These interactive materials should exhibit self-regulating properties to allow for autonomous switching between states. Thus, different states are able to ‘sense’ one and other and can communicate and influence the generated output.

In this progress report, we will focus on macroscopic polymeric materials, those you can see with the naked eye, touch or hold. We will highlight promising stimuli-responsive materials, some of which already show interactive behavior, alongside others which would require minor adaptations or further development to become interactive. Each section will primarily focus on a single stimuli however, more advanced systems often make use of coupling multiple stimuli. Many of the systems detailed below make use of supramolecular interactions and elegantly demonstrate how these interactions often represent the essential driving force to yield materials with a certain function. Although a plethora of other materials based on nanoparticles (NPs), vesicles, supramolecular polymers, inclusion com-

plexes etc. do exist, they have been deemed beyond the scope of this progress report.

## Aqueous Stimuli-Responsive Materials

### Thermoresponsive Materials

Temperature- or thermoresponsive materials are widely known to undergo a volume-phase transition at certain lower or upper critical solution temperatures (LCST or UCST).<sup>[6]</sup> Above the LCST or below the UCST, polymer chains transform from being well solvated in solution into collapsed aggregates. Often referred to as a sol-gel transition this phenomenon is driven by the hydrophobic effect in water, where polymer-polymer interactions dominate over polymer-solvent interactions. From a thermodynamic perspective, the entropic contribution (exclusion of water molecules from the swollen networks or solvated polymer chains) overcomes the enthalpic gain that arises from hydrogen bonds between water and the polymer chains.<sup>[7]</sup> First reported in 1968 by Heskins and Guillet, poly(*N*-isopropylacrylamide) (PNIPAAm) is undoubtedly one of the most popular thermoresponsive polymers.<sup>[8]</sup> Its LCST is 32 °C and depends on the hydrophilicity of the polymer backbone.<sup>[9]</sup> Hence, incorporating hydrophobic or hydrophilic comonomers into the polymer chain helps to tune the LCST to higher or lower temperatures as desired.<sup>[10]</sup> In 2012, Rotzetter et al. used PNIPAAm hydrogel sheets as “sweating surfaces” for the roof of a model

house, Figure 2.<sup>[11]</sup> Irradiation with light from a solar simulator ( $1000 \text{ Wm}^{-2}$ ) caused the surface to heat up. Above the LCST the PNIPAAm surfaces contracted and expelled the incorporated water. Upon further irradiation, the expelled water evaporated from the PNIPAAm surface. As a result, the temperature of the model roof was maintained at room temperature over the course of 3 h. This example shows how a well-known thermoresponsive polymer could be used in an elegant way to passively cool buildings. If this material was placed in a real world setting, it would possess all the requirements to function as an interactive material. Belal et al. reported a three-component supramolecu-

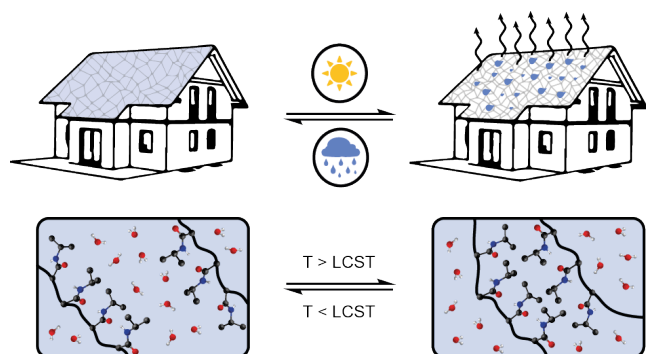


**Figure 2** PNIPAAm hydrogel sheets as “sweating surfaces” on a model roof. In temperatures above the LCST, the surfaces expel stored water in the roof which cools the building through the endothermic evaporation process.<sup>[11]</sup>

lar hydrogel, which became swollen at temperatures above the polymer LCST.<sup>[12]</sup> The hydrogel was based on pol(*N,N*-dimethylacrylamide) functionalized with naphthalene (Np) guest units. Introduction of the tetracationic cyclophane host cyclobis(paraquat-*p*-phenylene) (CBPQT<sup>4+</sup>) resulted in significant swelling of the system on account of complexation between CBPQT<sup>4+</sup> host and Np guest. Incorporation of a tetrathiafulvalene (TTF)-endcapped PNIPAAm then introduced temperature-induced swelling to the hydrogel. At  $T < \text{LCST}$ , TTF preferentially bound to the CBPQT<sup>4+</sup> however, when heated above the LCST the TTF-based polymer collapsed resulting in decomplexation of the TTF unit. The uncomplexed CBPQT<sup>4+</sup> was then able to diffuse through the gel and subsequently bind the hydrophobic pendant Np guests. Complexation of the Np by CBPQT<sup>4+</sup> shields the hydrophobic guest, which results in swelling of the gel. On account of charge-transfer interactions, the complexes of CBPQT<sup>4+</sup> with either Np or TTF had distinctly different colors. Additionally, alternative thermoresponsive polymers allowed for tuning of this transition temperature. If cargo could be released or captured as a result of the swelling/deswelling process and the temperature could be linked to a physiological process, then the system would be closer to achieving interactive behavior.

Smart windows represent another domestic application for thermoresponsive polymers. The materials' phase transition is used to switch between a transparent and a translucent state of the window, hence, modulating the intensity

of incoming light. Changing the hydrophilic/hydrophobic balance allowed for the UCST of polyampholyte hydrogels to be tuned between 25-55 °C.<sup>[13]</sup> Similarly, the LCST of hydroxypropyl cellulose was tuned between 30-50 °C through addition of glycerol, which at the same time served as an anti-freezing agent.<sup>[14,15]</sup> Poly(ethyleneglycol) (PEG) usually exhibits a LCST of 52 °C and can mediate thermoresponsive behavior in materials. In a report published in 2016, PEG-functionalized with perylenebisdiimide (PDI) units were used to self-assemble into fibers in aqueous media.<sup>[16]</sup> Changing the PEG-terminus from a methoxy to an ethoxy group caused the LCST for the respective PDI derivative to drop from 51 to 26 °C and thus mixed ratios of the two PDIs enabled tuning the LCST of the system over that range. The resulting fibers formed non-fluorescing hydrogels in water. Above the LCST, these fibers broke up into columnar nanostructures and formed a biphasic liquid crystal (LC)/water mixture that exhibited bright red color and strong fluorescence.

As thermoresponsivity is often related to shrinking or swelling of hydrogels, it has been used to promote motion in smart actuators. Seminal examples of hydrogel-based actuators are highlighted below. A dual-thermoresponsive material was reported by Hessberger et al., composed of amphiphilic Janus hydrogel rods with a LC elastomer tail and a PNIPAAm head.<sup>[17]</sup> When added to a toluene-water mixture, these Janus rods self-assembled at the liquid-liquid interface with the PNIPAAm-based heads pointing towards the lower aqueous layer. Using this approach, thin films of the rods were fabricated and demonstrated actuating behavior over a broad temperature range. The LC elastomer component underwent shape changes via nematic-isotropic phase transition (40-100 °C), while the PNIPAAm component exhibited volumetric expansion below its LCST (32 °C). As a result, four distinct particle shapes could be formed over a temperature range of 80 °C (20-100 °C).

Zhang et al. demonstrated an elegant combination of coupled light- and thermoresponsive behavior through depositing a thin Au layer on a NIPAAm-based hydrogel ribbon.<sup>[18]</sup> Upon irradiation with IR-light, Au plasmon resonance produced heat, which was transferred interfacially to the hydrogel resulting in anisotropic shape change of the gel. Within milliseconds, helical ribbons were switched between left and right-handed orientation using pulsed laser light. A NIPAAm-based composite hydrogel with cofacially embedded titanate(IV) nanosheets was reported by Kim et al.<sup>[19]</sup> The titanate nanosheets were negatively charged, and thus showed strong repulsion when brought together. Upon phase transition and collapse of the PNIPAAm network, this repulsion lead to excessive uniaxial stretching of the hydrogel. This anisotropic shape change was used to mediate motion. Such composite materials are in high demand and have attracted significant public and scientific interest, as they combine soft matter with electrical, optical and mechanical properties of nanoparticulate components.

Another actuating composite material has been reported

by Xie et al.<sup>[20]</sup> The authors developed shape memory implants based on near-IR active black phosphorous sheets in a polyurethane (PU) matrix. Casted films of this composite material folded above the glass transition temperature of PU and remained static below. Upon irradiation with light at 808 nm, the black phosphorous sheets produced heat, triggering a transition from a glassy to amorphous state and causing the specimen to unfold and return to its original shape. Maggini et al described Eu(III)-decorated fluorescent carbon nanotubes that were magnetically aligned in a NIPAAm precursor solution prior to polymerization.<sup>[21]</sup> The resultant polymerized materials showed anisotropic absorption/emission behavior and intensities on account of (i) the alignment of the functionalized carbon nanotubes and (ii) in response to temperature-triggered phase transition. In the area of electrochemical energy storage devices, Shi et al. proposed a temperature-switchable capacitor based on the sol-gel transition of pluronics in water.<sup>[22]</sup> Above 20 °C, the sol-gel transition occurred and previously mobile ions became entrapped within the gel leading to a resistance increase and eventually interruption of the electrical circuit. Anisotropy plays an important role in the described materials, whether it concerns the hydrogel shape or internal alignment of the nano-objects.

## Photoresponsive Materials

Materials with embedded switches that respond to light were amongst the first responsive materials to be reported.<sup>[23,24]</sup> Photoswitches are a particularly attractive tool as the stimulus, light, can be applied with both temporal and spatial control and modified through light intensity, wavelength and irradiation time.<sup>[25–27]</sup> As a result, there are a plethora of reports demonstrating the responsive behavior in the fields of drug delivery, 3D printing, sensing, microscopy and information technology.<sup>[28–33]</sup> Current established photoresponsive materials consist of a chromophore that can convert a light input into a number of potential chemical outputs. The exact response from the chromophore depends on the designed structure and the irradiation wavelength of light used. The rapid response times, high atom efficiency and often reversible nature between photoswitchable states make these systems attractive from an environmental perspective.

Photoresponsive materials can be categorized based on the type of synthetic chemical transformation that the chromophore undergoes. Typical transformations include tautomerization, (photo)cleavage, cyclizations, dimerization, polymerization, cycloadditions and *cis-trans* isomerizations.<sup>[34–37]</sup>

Aqueous photoresponsive systems that exhibit reversible isomerizations have been largely focused on azobenzene derivatives. One of the first reports was published by Sugiyama et al. in 1968, who synthesized azobenzene- and thiazene-functional polymers that were responsive to light.<sup>[38]</sup> Aida and co-workers developed an elegant water-soluble adhesive photoswitch, which selectively binds to a target enzyme with photochemically tunable activity (Fig-

ure 3A).<sup>[39]</sup> The central azobenzene unit carried a sulfonamide (SA) on one side and polymer-bound guanidine units that acted as a “glue” on the other. The former inhibited the carbonic anhydrase (CA) active site, while the latter targeted the enzyme surface through multiple electrostatic interactions. The SA moiety, upon docking at the CA active site, guided the connecting glue to an oxyanion-rich area in proximity to the active site for adhesion, ensuring conjugation between glue and CA (Figure 3A). In this geometry, the isomerization of the azobenzene unit generates a push–pull motion of SA, resulting in its docking and undocking at the active site of CA with the help of a competing substrate.

Huang et al. reported an ion-conducting supramolecular hydrogel based on alpha-cyclodextrin ( $\alpha$ -CD), an azobenzene unit and ionic liquid which were grafted onto a gel matrix.<sup>[40]</sup> The resulting gel was photoresponsive on account of the different association constants between *cis*- and *trans*-azobenzene derivatives towards  $\alpha$ -CD. Irradiation with light at 365 nm lead to the formation of *cis*-azobenzene which had a lower binding affinity to  $\alpha$ -CD compared to the *trans* isomer. As a result,  $\alpha$ -CD preferentially bound to the anionic component of the ionic liquid and the resistance of the hydrogel increased on account of decreased ion mobility. The more stable  $\alpha$ -CD *trans*-azobenzene complex was readily reformed by irradiating with light at 420 nm. This released the anionic component of the ionic liquid which increased ion mobility and decreased resistance. A logic gate was also embedded within the hydrogel, which allowed it to reversibly switch ON and OFF an electrical circuit though irradiation with light.

There are a number of reversible photosensitive reactions, which have been implemented as cross-linking units within materials based on cycloadditions. Anthracene, for example, undergoes a reversible [4+4] cycloaddition using >350 nm light, which reverts to its original structure upon irradiation with UV light <350 nm or using heat. Biedermann et al. used an anthracene derivative, which bound to the macrocycle cucurbit[8]uril (CB[8]) in a homoternary (2:1) fashion to form hydrogels.<sup>[41]</sup> Through post-functionalization of hydroxyethyl cellulose (HEC) with the anthracene guest molecules, self-assembly in water yielded hydrogels with dynamic cross-links. Encapsulation of the anthracene guests within the CB[8] cavity resulted in 10-fold rate enhancement of the photodimerization in water.

The same concept was used to develop hydrogels with bio-relevant and reversibly tunable moduli with hyaluronic acid (HA) backbones. Exploiting the supramolecular homoternary complexation of coumarin derivatives to CB[8], stiffening of physically cross-linked hydrogels was mediated by [2+2] photodimerization of the encapsulated coumarin moieties, this process was reversible for one cycle.<sup>[42]</sup> Under the tested conditions, stiffening with coumarin-functionalized HA was more reversible than coumarin-functionalized HEC. The mechanisms by which polysaccharides like HEC can retard the photo-reversible properties of coumarin and anthracene remain unidentified. This

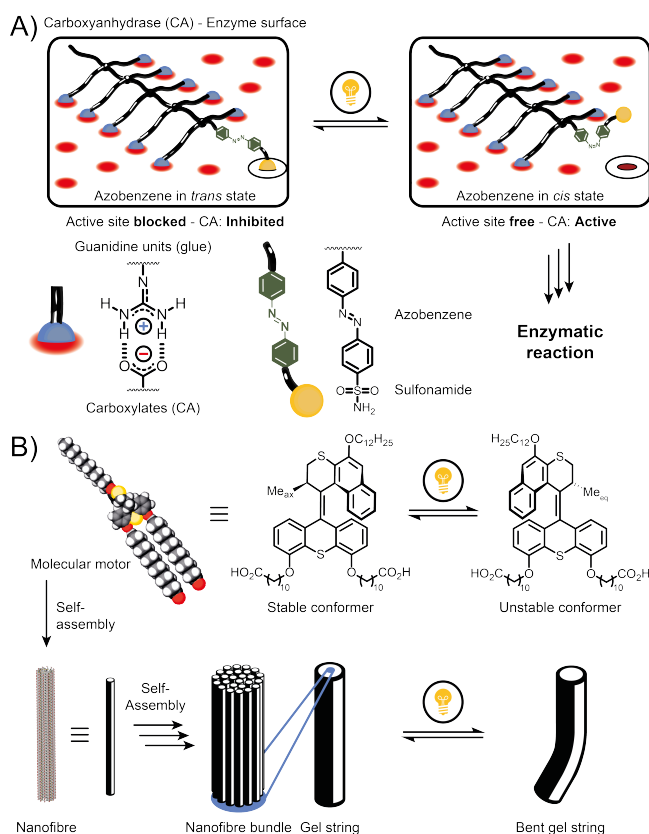


**Figure 3** A) Schematic representation of the adhesive photoswitch. Guanidine units interact with carboxylates on the carboxyanhydrase enzyme surface and act as glue. When existing as the *trans*-azobenzene isomer, the connected sulphonamide unit binds and blocks the active site of CA. Isomerization to the *cis*-isomer generates a push-pull motion that undocks SA from the binding site and thus increases the enzyme activity. B) Schematic of the photoresponsive rotary motor and its self-assembly into nanofibers reported by Feringa and co-workers. The nanofiber-containing solution is manually drawn from a pipette into a  $\text{CaCl}_2$  solution to achieve unidirectional alignment in bundles, generating a hydrogel string that is able to bend upon exposure to UV irradiation. Bending is achieved through photochemical and thermal helix inversion steps through an unstable intermediate.<sup>[45]</sup>

allowed for switching between covalent and non-covalent states, while maintaining a homogenous chemical composition throughout the network. This concept was further developed by Webber and co-workers, who used [2+2] photodimerization of *trans*-Brooker's Merocyanine to switch between supramolecular and covalent hydrogels.<sup>[43]</sup>

A [4+4] photodimerization was used by Anseth and co-workers for on-demand stiffening of 8-arm PEG matrices.<sup>[44]</sup> The authors created cytocompatible hydrogels with moduli, which could be tuned within a range of 10 to 50 kPa by irradiation with light at 365 nm. The location of NFAT, a downstream target of intracellular calcium signalling, could be monitored on account of its moduli-dependent movement. The authors reported that NFAT translated to the nucleus when the hydrogel stiffened. In contrast, NFAT remained in

the cytoplasm when cultured on hydrogels with static moduli. This work demonstrated how networks with altering stiffness could be used to investigate mechanoresponsive cell signaling pathways. These materials therefore could serve as important model systems for understanding cell signalling responses.

Feringa and co-workers reported a photoresponsive amphiphilic molecular motor exhibiting chirality.<sup>[45]</sup> UV light (365 nm) switched the molecular motor from a stable to a less stable isomeric state, which resulted in an unfavored, strained geometry driving the back reaction and simultaneously releasing heat. In an aqueous environment the chiral molecules self-assembled into a helical nanofiber. Subsequent transfer of these aggregates into a  $\text{CaCl}_2$  solution drove the nanofibers to assemble into bundles which yielded macroscopic hydrogel strings. When irradiated, these artificial muscle-like strings bent towards the light source (in air or water) at a considerable rate of approximately  $1.5^\circ \text{ s}^{-1}$  (Figure 3B). This process however, required almost 3 h of incubation at  $50^\circ \text{ C}$  to return to its original state, which is substantially longer recovery than biological muscles experience for example. Furthermore, the system's applicability is limited, as its reversibility declines with each cycle. This was attributed to the instability of the hydrogel strings at  $50^\circ \text{ C}$ , the temperature required for the inversion process.

Photothermal therapy (PTT) exploits NPs delivered to tumors that can be excited by an externally-applied laser.<sup>[46,47]</sup> On account of their inherent biocompatibility, simple bioconjugation chemistries and efficient near-IR light-to-heat conversion, Au and Pt NPs have typically been used. Hughes and co-workers developed hydrogels from agarose and 2-(methacryloyloxy)ethyl trimethylammonium chloride (METAC)-functionalized Au NPs.<sup>[48]</sup> Plasmon resonance led to an increase in temperature ( $>45^\circ \text{ C}$ ) of the hydrogel matrix. Subsequently, a temperature-dependent softening and an enhanced diffusion of an encapsulated cargo into the surrounding environment was observed. The system was able to release a number of anti-VEGF compounds including monoclonal antibodies and proteins, while maintaining their stability. In addition to the NPs' properties, their transparency made them ideal for use in ocular implants.

Controlled release using visible light as a trigger is becoming increasingly popular, shifting away from traditional UV stimuli. Wang et al. recently designed a protein-based hydrogel that was based on polymerized CarH<sub>c</sub> proteins using SpyTag-SpyCatcher chemistry.<sup>[49]</sup> If the CarH<sub>c</sub>-containing polymers were exposed to AdoB<sub>12</sub> (an adenosylcobalamin) in the dark, the CarH<sub>c</sub> domains formed tetramers, generating a stable hydrogel. Upon irradiation with green (522 nm) or white light, these tetramers rapidly disassembled leading to dissociation of the gel. The authors designed the hydrogel to encapsulate and release/recover cells within the 3D culture matrix. This light-induced process recovered  $90 \pm 7\%$  of 3T3 fibroblasts and  $88 \pm 5\%$  of viable mesenchymal stem cells.

## Electroresponsive Materials

Electroresponsive materials include those that show a macroscopic response (e.g. shape change) upon subsection to an electric field and are generally based on electroactive polymers (EAPs). EAPs include polyelectrolytes, conductive polymers or polymers with polarizable functionalities.<sup>[50]</sup> Although electroresponsive materials have been used as drug delivery vehicles and sensors, one of the most prominent applications lies in the fabrication of smart actuators towards soft robotics and artificial muscles.<sup>[51,52]</sup>

One of the early examples of an electroresponsive actuating system was reported in 1982, where a partially hydrolyzed acrylamide gel underwent a phase transition upon application of an electric field across the gel.<sup>[53]</sup> The degree of volume change was reported to be as large as 500-fold and the transition was associated with free acrylic acid groups within the network. The reorganization of mobile ions created osmotic pressure gradients throughout the gel, resulting in uniaxial stress towards the positive electrode and hence deformation.

As many of the systems reported are directed towards biomedical applications (as artificial muscles or implants), their use in an aqueous physiological environment remains crucial. As such, polyelectrolytes represent an attractive platform and corresponding hydrogels are easily prepared in aqueous media after reaching an equilibrated swollen state. Examples include copolymers that contain either negatively-charged moieties (e.g. sulfonic acids, carboxylic acids) and/or alkylammonium functionalities (e.g. dimethylaminoethyl acrylamide) as pendant groups to the polymer backbone. Recent examples have shown that corresponding hydrogels are readily actuated via periodic application of an electric field (0.01–0.1 M NaCl, 5 V cm<sup>-1</sup>), depending on the shape of the mold these hydrogels are able to perform unidirectional movement and can transport cargo.<sup>[54,55]</sup>

In further development of this area, electroactive nanocomposites have been explored. Yang et al. homogeneously dispersed reduced graphene oxide (rGO) nanosheets within a hydrogel matrix containing 2-acrylamide-2-methylpropanesulfonic acid (AMPS) moieties.<sup>[56]</sup> Fine-tuning of the respective charge ratios and the amount of rGO sheets in the system resulted in high conductivities and strong osmotic pressures. The latter enabled reversible, rapid bending and large volume changes upon deswelling/swelling. The rGO-doped hydrogels exhibited bending behavior that increased by 180% compared to a control gel without any rGO incorporated (0.01 M NaCl, 10 V cm<sup>-1</sup>).

In another study, Al(OH)<sub>3</sub> NPs were embedded in an acrylamide-based hydrogel matrix.<sup>[57]</sup> The nanocomposite showed remarkably high tensile strength (up to 2 MPa), which was found to be dependent on the Al(OH)<sub>3</sub> NP content. The authors reported bendable actuators (Figure 4A) that were able to move bidirectionally upon change in the direction of the electric field (0.5 M NaCl, 15 V cm<sup>-1</sup>). The nanocomposite hydrogels showed interesting mechanical ca-

pabilities and, upon electrical stimulus, could lift a target object made of PDMS (0.5 g) 20 times its own weight. The bidirectional behavior however, is slightly overshadowed by an irreversible shape change of the initial polyelectrolyte hydrogel. Application of an electric field towards the straight, pristine hydrogel resulted in bending, leading to a concave shape (Figure 4A, pathway a). Upon reversing the electric field however, the hydrogels did not change from a concave to convex shape (pathway b), rather they “bent back” as attractive forces were mirrored (Figure 4A, pathway c). The irreversible shape change represents a clear limitation for this system. Complete reversibility between the two shapes of these hydrogel strips would be highly desirable (Figure 4A), for applications such as hydrogel “forceps” this reversibility is not necessary (Figure 4B). Ideally, future developments will show improved mechanical properties and bending behavior. Furthermore, nanocomposite materials will provide access to actuators with higher work loads, lower activation voltages, high bending strains, improved response times and simultaneously possess good biocompatibility.

In addition to classic polyelectrolyte systems, Ozaki et al. demonstrated host-guest self-assembled systems that reveal interesting properties upon application of an electrical stimulus.<sup>[58]</sup> The authors used cycloparaphenylenes (CPP) as macrocyclic hosts to incorporate dimeric iodine. The presented crystal structure shows uniaxial alignment of this host-guest complex yielding tubular-like CPP-iodine assemblies. Application of an electrical bias lead to the formation of polyiodide chains with an increase in electronic conductivity on account of charge transfer between CCP and iodine moieties, which resulted in white light emission. Although this study lacks mechanistic insight, these materials hold promising potential for future energy and light-emitting applications.

Electrorheological fluids (ER) have emerged as their own disciplinary subfield within the area of electroresponsive materials. ER fluids are dispersions (in an insulating medium) of semi-conducting particles or polarizable molecules that align on application of an electric field. This alignment enables switching between liquid- and solid-like behavior with extremely fast response times and a concomitant change of mechanical properties. An in-depth discussion on these materials was deemed beyond the scope of this perspective as (i) they currently do not include gel-like materials in aqueous media, and (ii) Choi et al. recently published two comprehensive reviews detailing the general field and recent developments.<sup>[61,62]</sup>

## Magneto-responsive Materials

Magneto-responsive materials typically consist of polymer solutions or networks, which are doped with magnetic NPs. Generally, superparamagnetic species ( $\gamma$ -Fe<sub>2</sub>O<sub>3</sub> or Fe<sub>3</sub>O<sub>4</sub>) are combined with a polymeric matrix to form composite materials, which respond to weak, static or alternating magnetic fields. Amongst these materials, fer-

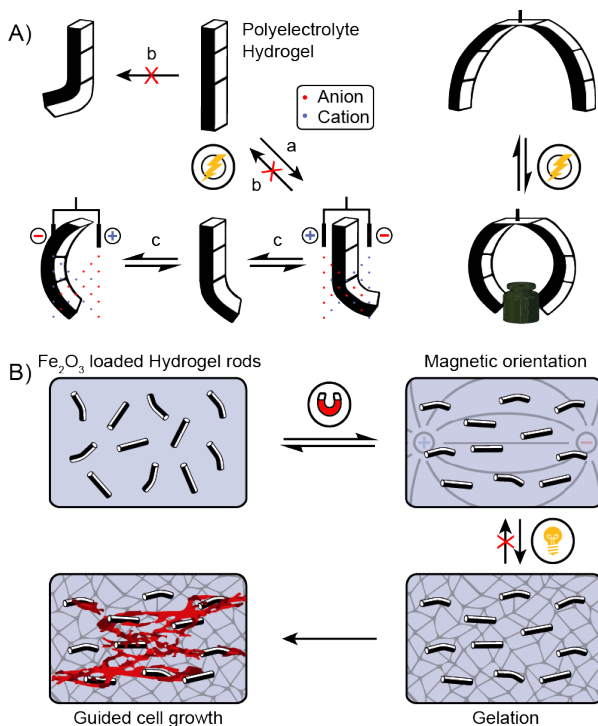


**Figure 4** A) Electro-actuation of an acrylamide gel containing  $\text{Al}(\text{OH})_3$  NPs.<sup>[57]</sup> B) Reversibly electroresponsive hydrogel “forceps”. C) Reversible magnetic alignment of  $\text{Fe}_2\text{O}_3$  nanorods for the unidirectional regeneration of nerve cells.<sup>[59,60]</sup>

rogels, hydrogels with embedded ferromagnetic particles, hold potential for applications in biomedicine, as smart actuators or sensors and soft robotics.<sup>[63–65]</sup> In the literature, magneto-responsive materials have mainly been utilized in two ways, as single responsive materials and in coupled systems. For single responsive materials, application of a magnetic field can cause orientation, deformation, bending, swelling/deswelling or even translation through space.<sup>[66]</sup> For coupled magneto/thermo-responsive materials, alternating magnetic fields are applied to remotely create localized heat within a system, which has been especially useful for drug targeting applications.<sup>[67,68]</sup>

One of the first reports in 1996 by Zrinyi et al. investigated the deformation of polyvinylalcohol-based ferrogels using a non-uniform magnetic field.<sup>[69]</sup> Subsequently, substrates including synthetic polymers (e.g. polyacrylamide),<sup>[70]</sup> LC elastomers,<sup>[71]</sup> natural polymers (alginate,<sup>[72]</sup> chitosan,<sup>[73]</sup> gelatin<sup>[74,75]</sup>) alone or as part of composite materials (e.g. with cellulose nanocrystals) have been used to obtain ferromagnetic materials with remarkable magnetic response times and properties.<sup>[76–78]</sup> To mediate gelation in ferrogels, several strategies can be employed. Conventional covalent cross-linkers have been used to entrap and immobilize ferromagnetic particles within the network.<sup>[79]</sup> In a different approach, the surface of iron oxide NPs was modified with (amphiphilic) polymer chains. The resultant NPs formed gels via entanglement of polymer chains<sup>[80]</sup> or microphase separation of individual poly-

mer blocks at the NP surface.<sup>[81]</sup> While most of these examples highlight the material or magnetization properties, only a handful have introduced concepts towards smart applications, some of which are highlighted below.

Lin et al. proposed a coupled magneto/thermo-responsive hydrogel for switchable molecular sieving.<sup>[82]</sup> The authors reported PNIPAAm hydrogels embedded within an iron oxide NP-loaded poly(ether sulfone) matrix. Casted membranes of these materials were responsive to alternating magnetic fields that created localized heat to trigger PNIPAAm phase transition. This thermoactivation caused the nanogel channels to collapse, and thus opened pores with a molecular weight cut-off of 1750 kDa, as demonstrated by dextrane ultrafiltration tests. De Laporte and coworkers made use of magnetic orientation to develop an injectable hydrogel system for use in the treatment of spinal cord injuries.<sup>[59,60]</sup> The authors dispersed rod-shaped hydrogels or short fibers with immobilized iron oxide NPs (down to 0.005 vol% loading) in a gel precursor solution for injection. Before bulk gelation was induced, the rod-shaped microgels were aligned via application of a weak magnetic field (Figure 4C). The study showed that embedded nerve cells preferred unidirectional growth over random proliferation, if the microgels were aligned. In its current form, the cross-linking of the surrounding matrix is currently irreversible (Figure 4C). Rendering this cross-linking process reversible would lead to an interactive material. A scenario in which the cells degrade the matrix again would enable cycling between magnetic (re-)orientation of the hydrogel rods and subsequent re-curing of the surrounding matrix. As these selected publications highlight, simple chemical concepts can impart significant effects towards their environment. Since the human body can be exposed to magnetic fields and field gradients without harm, it is expected that magneto-responsive materials will attract more attention within the growing area of biomedical applications.

## Chemoresponsive Materials

Use of chemical stimuli to program function into materials is a rapidly growing area of responsive materials, owing to the vast array of applications within sensing, molecular machines, actuators, tissue engineering, electronics, and drug delivery.<sup>[85–88]</sup> Chemoresponsive materials refer to systems that are chemically transformed upon introduction of small or large molecules such as gases, proteins, enzymes or antibodies. A common strategy to implement chemical responsiveness into a material is through the addition of redox-active moieties. Redox-responsive materials have the ability to self-assemble and disassemble upon a change in their redox states. Van der Boom and co-workers reported the preparation of colored nanofilms based on a new spin-coating methodology.<sup>[89]</sup> The authors created alternating layers by spin-coating solutions of metal polypyridyl complexes and a Pd(II) salt on a range of rigid and flexible substrates. The resultant electroactive redox-responsive films

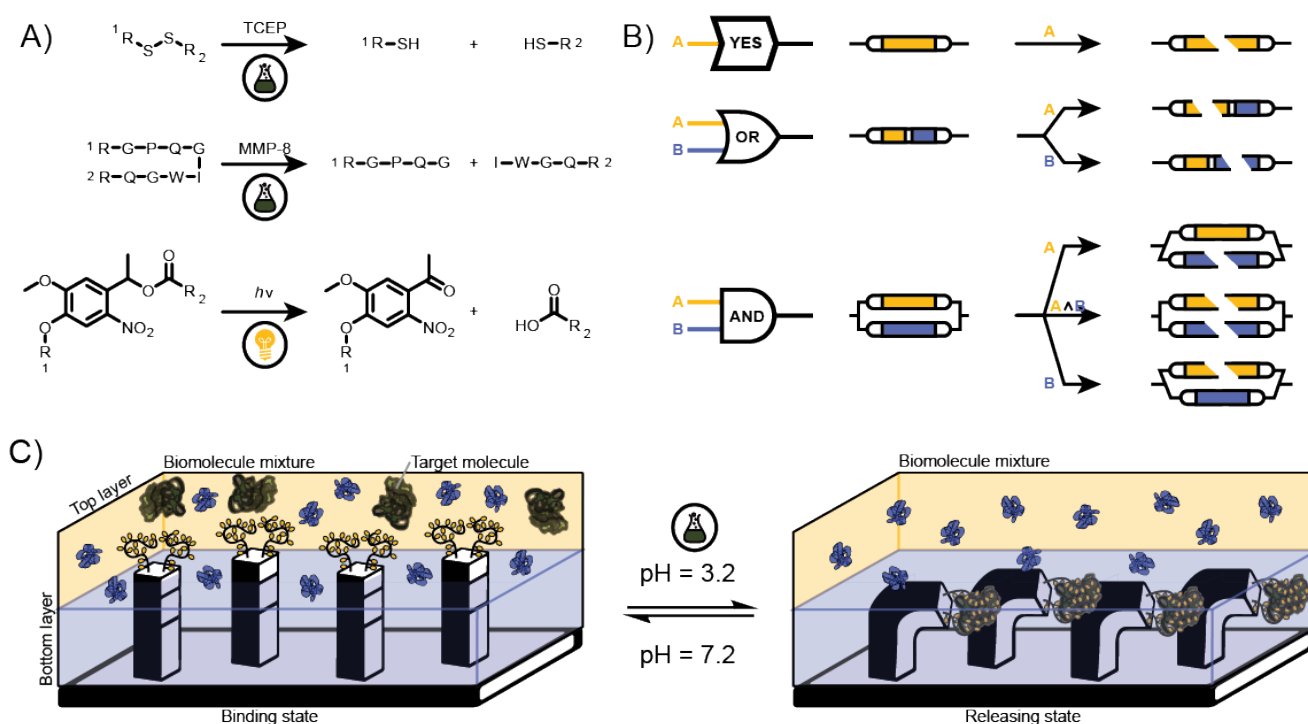


**Figure 5** A) Reactions resulting in cleavage of the stimuli-responsive groups: disulfide bonds, the MMP cleavable sequence and the photocleavable *o*NB moiety. B) YES, OR and AND-gates for Boolean logic-gated responsive materials.<sup>[83]</sup> C) Scheme depicting the biphasic microfluidic chamber with aptamer-decorated microstructures. The upper fluid layer is used to introduce biomolecule mixtures. In the presence of a solution of pH 7.2, the hydrogel in the lower layer swells and the aptamer-fingers protrude into the top solution, allowing for 'catching' of the target molecule. At pH 3.2, the hydrogel contracts, bending the fingers into the bottom layer, resulting in denaturation of the aptamer and 'release' of the captured biomolecules.<sup>[84]</sup>

had a high chromophore density. As range of intensities and colors could be accessed through changing the metal cation of the polypyridyl complex (Os/Ru/Fe), the ligand used as well as through mixing different complexes together. Further control over the color efficiency was achieved through adjusting the number of deposition cycles or through application of an electrical potential. The materials produced had favorable ON/OFF ratios, good electrochemical stability and coloration efficiencies in addition to enhanced homogeneity and significantly faster coating times. These advantages rendered this approach a highly attractive alternative for the facile production of electrochromic coatings. To the best of our knowledge, the first report of a water-based material, which was responsive to a chemical stimuli (other than a redox system) was reported by Katchalsky and co-workers in 1970.<sup>[90]</sup> The authors devised a collagen fiber and used a salt solution as fuel to produce mechanical work directly from chemical energy.

The Harada group used the ferrocene/ferrocenium (Fc/Fc<sup>+</sup>) redox couple to self-assemble molecular building blocks into hydrogel networks.<sup>[91]</sup> Initially, Harada and co-workers utilized the switchable redox properties of a Fc derivative tethered to a polymeric backbone. Two complementary acrylic acid-based polymers were synthesized, the first with pendant Fc, the second with pendant beta-cyclodextrin ( $\beta$ -CD) units. This allowed controlled self-

assembly into a hydrogel through complexation between the pendant complementary Fc and  $\beta$ -CD. The redox state of Fc dramatically alters its binding affinity to  $\beta$ -CD. Upon reduction, Fc has an increased binding affinity with a  $K_a$  value of  $1.1 \times 10^3 \text{ M}^{-1}$  that induces host-guest complexation between Fc and  $\beta$ -CD. This causes the polymer chains to form a hydrogel at 2 wt% with a modulus of  $G' = 176 \text{ Pa}$ . The oxidized Fc<sup>+</sup> has a reduced binding affinity to  $\beta$ -CD, which results in dissociation of the host-guest complex accompanied by a gel-to-sol transition. A control experiment, whereby an adamantane derivative (Ada) with a higher binding affinity ( $K_a = 3.5 \times 10^4 \text{ M}^{-1}$ ) was introduced to the system resulting in the same gel-to-sol transition as the more stable  $\beta$ -CD Ada complex was formed. Alternatively, reduction of the Fc<sup>+</sup> through addition of a chemical oxidant (glutathione) or thermal treatment (50 °C, 1 h) resulted in dissociation of the network.

The same group subsequently reported the macroscopic self-assembly of polymeric hydrogels.<sup>[92]</sup> These networks contained either pendant  $\beta$ -CD, Fc or styrenesulfonate groups. In the reduced state, the Fc gel exclusively interacted with the  $\beta$ -CD-containing gel. Conversely, under oxidative conditions, Fc<sup>+</sup> was bound to the anionic sulfonate gel. The authors were able to form an ABC type assembly through partial oxidation of the Fc-functional hydrogel. This demonstrates how a multicomponent system can exhibit bulk

changes at the macroscopic level in response to changes at the molecular level.

In a more recent example, injectable cyclic progelator peptides were used for tissue scaffolding to promote cardiac function by Gianneschi and co-workers.<sup>[93]</sup> The cyclic peptides contained an inactive gelling sequence, a cleavable recognition sequence (recognized by two different enzymes) and a simple disulfide bridge. When delivered via a minimally invasive cardiac catheter, the cyclic peptides were ring-opened by an endogenously expressed inflammatory enzyme present in the heart, which activated the incorporated gelation sequence. The linear peptides then self-assembled into  $\beta$ -sheet fibrils generating a peptide-based hydrogel at 37 °C.

Matrix metalloproteinase (MMP) responsive materials for cargo release have experienced increased popularity since their introduction into synthetic matrices in 2003.<sup>[94]</sup> Recently, Karp and co-workers developed an arthritis flare-responsive delivery system using a MMP degradable triglycerol monostearate (TG-18) hydrogel.<sup>[95]</sup> The TG-18-based hydrogel was loaded with triamcinolone acetonide as a model drug. This material is particularly apt for biological delivery applications as TG-18 is both on the FDA list of generally recognized as safe (GRAS) compounds as well as being a hydrogelator that possesses an enzyme labile ester linkage, which can respond to inflammation.

Increased levels of complexity were introduced by De Forest and co-workers who created materials with Boolean logic gates such as YES, OR or AND events.<sup>[83]</sup> The inputs are serial or parallel combinations of enzyme, reductant and/or light-triggered dissociation reactions (Figure 5A). Seventeen synthetically complex and distinct hydrogels were designed using these logic gates to trigger stimulated drug release via partial or full degradation of the respective gels (Figure 5B). While elegant in its design, the considerable synthetic challenge of incorporating complex logic gates into these hydrogels limits their application.

A simple and robust pH-responsive hydrogel was produced by Scherman and co-workers, who reported the production of hydrogels formed from three pentapeptide sequences based on the amino acids Isoleucine (I) and Aspartate (D): IDIDI DDII and DIID.<sup>[96]</sup> Upon addition of HCl, the concentration and charge distribution of the peptide sequence was altered. As a result, the molecular structure changes from fibrillar morphologies to entangled and interconnected  $\beta$ -sheets. The stiffness of the resulting hydrogels was shown to be tunable across two orders of magnitude (2-200 kPa). The formation of  $\beta$ -sheets in water is a powerful tool to mediate gelation, driven by supramolecular interactions.

Besenius and co-workers detailed multi stimuli-responsive dendritic peptide monomers comprising glutamic acid and methionine groups, which were able to self-assemble in water into  $\beta$ -sheets.<sup>[97]</sup> The authors were able to generate two chemical stimuli simultaneously using protons released from GOx-catalyzed and glucose-fueled reactions coupled to the production of

hydrogen peroxide. Through kinetic differences between the formation of  $\beta$ -sheets, an autonomous supramolecular polymerization was established. Gelation was observed at temperatures over 30 °C through the introduction of thermoresponsive triethylene glycol side chains at 0.7 wt% peptide content. The stiffness of the resulting gels could be controlled through altering enzyme (GOx) and glucose concentration, which dictated the lifetime and kinetics of the supramolecular assemblies formed. Responsive supramolecular gels have been fabricated by use of guanidiniocarbonyl pyrrole carboxylate (GCP) zwitterions. The zwitterions were conjugated to a benzene core in a tripodal fashion.<sup>[98]</sup> The resulting gelator formed stable aggregates between pH = 5-7 and deaggregated below (protonation) or above (deprotonation) these values, respectively. In subsequent work, this zwitterionic motif was bound to short aromatic thioethers, capable of forming fibrillar gel networks via  $\pi$ - $\pi$ -interactions. The multi stimuli-responsive supramolecular gels showed aggregation-induced emission at around 500 nm in the aggregated gel state and the fluorescence was quenched upon mechanical disturbance (vortexing), temperature increase (gel-sol transition) and pH variations.<sup>[99]</sup>

Aizenberg and co-workers recently reported a Self-regulated Mechanochemical Adaptively Reconfigurable Tuneable System (SMARTS).<sup>[100]</sup> The system consists of micro-structured hydrogel fingers, whose top surfaces were decorated with a catalyst. When the system was immersed in a bilayer, reversible swelling/deswelling caused a mechanical action moving the top surface of the hydrogel fingers in and out of the upper layer. As the upper layer contained specific substrates necessary for the catalytic reaction to proceed, the chemical reaction was turned ON when the structures straightened, and OFF when they bent. Additionally, self-regulation was provided through coupling the thermoresponsivity of PNIPAAm gels to a catalytic reaction of an exothermic nature, a “click” reaction between octylazide and phenylacetylene using Cu(PPh<sub>3</sub>)NO<sub>3</sub> as catalyst. Below the LCST of the PNIPAAm gel, the hydrogel swelled and the microfingers were straightened with their catalytic tips in the nutrient layer. Once the catalytic reaction occurred, heat was created thus increasing the temperature above the LCST. Consequently, a contraction of the hydrogel removed the catalytic fingers from the upper nutrient layer restarting the cycle in a continuous self-regulating fashion. On account of its self-regulating nature, this system is a true example of an interactive material, since both states A and B communicate and feedback information (Equation 2).

Further development lead to a similar system, which utilized aptamer-functionalized surfaces to carry out a catch-and-release processes (Figure 5C).<sup>[84]</sup> While immersed in the upper layer, the microfingers were able to selectively bind thrombin to the aptamer sequence and upon bending remove it. Unlike the previous thermoresponsive system, swelling and deswelling of the poly(AAc-co-AAm) hydrogel fingers was mediated via a pH change (pH < pK<sub>a</sub> = 4.25).

Under acidic conditions, acrylic acid groups were protonated, hydrogen bonding was suppressed and water was expelled from the contracted network. As a result, the decorated microstructures moved into the lower fluid layer. Simultaneously, binding of the aptamer was reversed under acidic conditions thereby releasing thrombin when  $\text{pH} < 5$ . The lower solution could be collected separately from the top layer enabling separation of the biomolecule mixture.

## Mechanoresponsive Materials

In contrast to chemo-, thermo- and light-responsive materials, the number of reported materials that show response to mechanical stress is limited. This is opposed to the plethora of mechanoresponsive materials known to exist in nature, which rely on conversion of mechanical forces at the macroscopic scale into chemical reactions at the microscopic scale. It is well known that mechanical forces can impart changes to the macroscopic properties (reactivity, conductivity, optical properties, etc.) of a material through augmenting the energetics of a chemical bond. The application of mechanical force within mechanoresponsive polymeric systems supplies the activation energy required for a chemical reaction to occur. Harnessing precise control for the design of mechanoresponsive materials with embedded function has, however been a challenge for researchers throughout the past two decades. In 2007, Wilson and co-workers used sonication as a means to exert a mechanical force, and causing the reaction of mechanically sensitive groups within the polymer chain.<sup>[101]</sup> This example was in contrast to previous reports, where mechanical force resulted in chain scission, however this took place in organic media. Translation of such approach to aqueous environments has been a challenge for material scientists.

A recent collaboration between the groups of Chen and Zheng resulted in a mechanoresponsive hydrogel with a spiropyran (SP) mechanophore embedded within the polymeric network.<sup>[102]</sup> Using Tween 80, methylacrylate- and SP-loaded micelles were polymerized in an oil-in-water emulsion. At the same time, the surrounding aqueous solution was polymerized into an acrylamide-based network encapsulating the SP-functional emulsion droplets. Upon application of mechanical force (as well as heat and UV light) SP could undergo a reversible structural transition between a ring-closed (SP) and ring-opened (merocyanine, MC) state, both of which had different optical properties. It was observed that under the application of an external mechanical force, the optical appearance of the hydrogel changed from pale yellow (SP state) to purple (MC state) and a corresponding change from green to red fluorescence was also observed. Interestingly, the system was reversible, reverting back to its original optical state upon irradiation with white light. The mechanical properties of the gel were also evaluated, the hydrogel was determined to be strong and tough with a tensile strength of 1.45 MPa, tensile strain of  $\approx 600\%$  and fracture energy of  $\approx 7300 \text{ Jm}^{-2}$ .

In 2019, Weder and co-workers reported the first

mechanoresponsive white light-emitting polymer network, which displayed reversible ON/OFF photoluminescence upon mechanical stretching and relaxation of the sample.<sup>[103]</sup> However, for prospective biomedical applications it would be desired to translate this material to an aqueous environment.

While the majority of synthesized materials become damaged and ultimately yield upon the application of mechanical stress; Gong, Nakajima and co-workers recently introduced a self-reinforcing hydrogel composed of a robust double network (DN), which stiffened upon application of an external mechanical force through mechanoradical polymerization.<sup>[104]</sup> The self-reinforcing gel was inspired by skeletal muscles, where repeated stress in the form of exercising leads to muscle growth. The rationale for using a DN hydrogel over a single network (SN) hydrogel was based upon the concentration of mechanoradicals that could be generated. Upon application of a mechanical force the polymer chains broke homolytically and yielded mechanoradicals. As these radical polymer chain ends are non-diffusive, they served as initiation sites for the generation of a separate interpenetrating polymer network (Figure 7A). The new functionality could be imparted at a desired position using spatially-programmed deformation. SN hydrogels are often weak and fail upon the application of mechanical force. A major challenge encountered in this work was to ensure a sufficiently high concentration of mechanoradicals formed without causing structural failure of the gel. Using the Fenton reaction as an indicator, the concentration of mechanoradicals in both DN and SN gels could be quantified. The number of radicals in the DN gels was an order of magnitude higher than in the SN gels. A spatial mechanoradical polymerization was trialed using PNIPAAm. A NIPAAm-loaded DN was locally compressed resulting in spatially confined polymerization, turning the stamped letters opaque and visible after heating above the LCST.

Walther and co-workers reported a Förster resonance energy transfer (FRET)-based tuneable mechanofluorescence DNA-based hydrogel with programmable sacrificial bonds and stress-relaxation behavior.<sup>[105]</sup> The authors reported facile construction of thermosetting and thermoreversible DNA hydrogels, which were extremely stretchable ( $>500\%$  elongation at break). The introduction of DNA tension probes to the pristine DNA network allowed for programmable force sensing and quantification of strain. At rest, the hydrogel was in a FRET-quenched state as the fluorophore and the quencher were in close proximity, Figure 7B. Stretching of the hydrogel broke the sacrificial duplex of the mechanosensing module, which separated the red light-emitting fluorophore from the quencher and decreased FRET. As a result, an increase in fluorescence was observed. Insight into the fluorescence increase upon application of mechanical force was found to be dependent on the topology of the hydrogel network and was less affected by the mechanophore architecture. Conversely, the orientation of the mechanophore during relaxation was found to dictate its

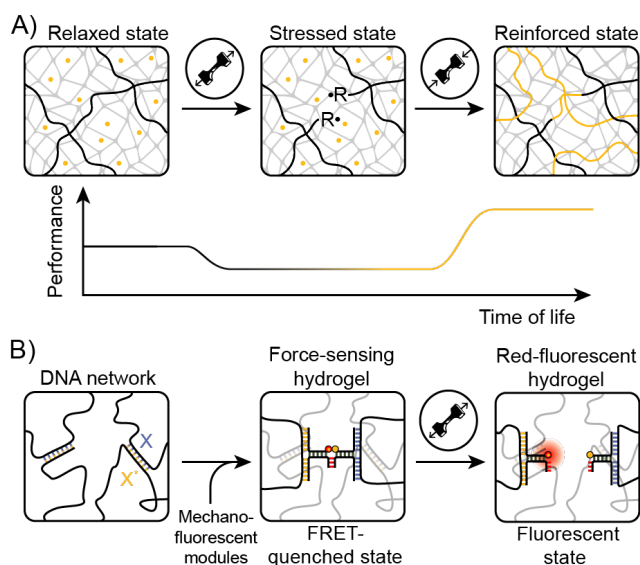


**Figure 6** A) A self-reinforcing hydrogel formed from a double-network. Mechanical stress leads to breakage of the brittle network. The mechanoradicals generated at the broken ends trigger polymerization of monomers supplied from the external environment to form a new network.<sup>[104]</sup> B) Schematic showing the pristine mechanofluorescence DNA-based hydrogel and formation of the FRET-quenched state followed by the separation of the FRET pair and subsequent increase in fluorescence upon application of a mechanical force.<sup>[105]</sup>

response. Application of these mechanofluorescence DNA-based hydrogels to analyze complex strain fields and produce multiscale 3D maps of strain fields in both composite and homogeneous samples was demonstrated. Through this analysis localized freezing-induced strain patterns in hydrogels were unveiled.

## Switchable Wettability

Switchable wettability of surfaces and materials requires the existence of two distinct states that are reversibly interchanged by one or multiple external stimuli.<sup>[106]</sup> The first state exhibits superhydrophobic or superoleophobic properties, while the second state is of a superhydrophilic or superoleophobic nature. The degree of this oleo- or water affinity is commonly determined by measuring the contact angle of the respective liquid droplet on the surface in question. Superhydrophobic surfaces are defined by a contact angle of water higher than  $150^\circ$ , whereas superhydrophilic surfaces should exhibit contact angles lower than  $5^\circ$ .<sup>[107,108]</sup>

Switchable wettability has become a major topic in the field of smart materials, especially for applications in biomedicine, functional textiles and coatings that exhibit self-cleaning/self-repelling properties or water/oil separation. Recent reviews discuss the scientific directions and applications of switchable wettability in detail;<sup>[109,110]</sup> here, we will highlight recent examples from the literature. It is known that superhydrophobic/hydrophilic surfaces are best

obtained when chemical functionalization and surface topology are synergistically combined. Switching between two states can be achieved with a variety of stimuli thus yielding responsive materials.

The PNIPAAm phase transition has been used to switch between hydrophobic and hydrophilic environments.<sup>[111]</sup> The same concept was successfully introduced in a polymer decorated membrane to separate oil-in-water emulsions in a controlled way.<sup>[112]</sup> Alternative strategies to carry out oil/water filtrations have been reported by Li et al., who used pH-responsive membranes based on poly(4-vinylpyridine) copolymers.<sup>[113]</sup> Through deprotonation/protonation of the functional surfaces, different polarities and hence wettability states were readily achieved.<sup>[114,115]</sup> A chemoresponsive approach was reported by Lei et al., who used N,N-(diethylamino)ethyl methacrylate-based copolymers.<sup>[116]</sup> The diethylamino group is able to capture and store  $\text{CO}_2$  as an ammonium carbonate complex. In this state, the membrane was superhydrophilic, whereas removal of  $\text{CO}_2$  from the membrane via simple drying with  $\text{N}_2$  reversed it to its superoleophobic state. To access switchable wettability via a phototrigger, fabrics were decorated with fluorinated azobenzene moieties. Upon irradiation of the surface with UV light, the azobenzene switched from its *trans*- to *cis*-conformation and therefore surfaces changed from a superhydrophobic to superhydrophilic state.<sup>[117]</sup> Wettability states were fully reversible for at least 10 cycles.

In a purely supramolecular example, aqueous solutions of a telechelic PEG with an  $\alpha$ -PDI and an  $\omega$ -perfluorated alkyl chain were drop-casted on glass surfaces.<sup>[118]</sup> Aggregation of the perfluorinated units via hydrophobic interactions and PDIs via  $\pi$ - $\pi$ -stacking resulted in highly hydrophobic surfaces with enclosed crystalline PEG domains. Above  $60^\circ\text{C}$ , the crystalline PEG domains melted and the resulting amorphous PEG-dominated surface showed superhydrophilic behavior that was reversibly switched back to high hydrophobicity upon cooling. Many of the reported surface materials focus on the switchability between superhydrophobic and superhydrophilic properties. Switching between two wetting modes involves the exploitation of the lotus leaf and rose petal effects. The former provides the classic rolling effect, where water droplets roll off the surface at specific angles, while the latter inhibits movement of the water droplet, pinning it to the surface. Rolling or pinning phenomena have been found to mostly depend on the surface topology of the nanostructures. If sufficient space between nanopillar constructs exists, capillary forces allow the water droplet penetrate the interstitial cavities (Figure 7). This causes the surface to exert adhesive forces on the droplet, and hence, it is pinned to the surface. In case of sufficiently close proximity of the nanoconstructs on the surface, capillary forces are not able to promote adhesion, and the droplets roll off the surface as in the classic lotus leaf effect.

Several attempts have been made to switch between the two states, mainly by manipulating the surface topology using an electrical or magnetic field.<sup>[120,121]</sup> Only two recent publications highlight the use of stretchable surfaces, which

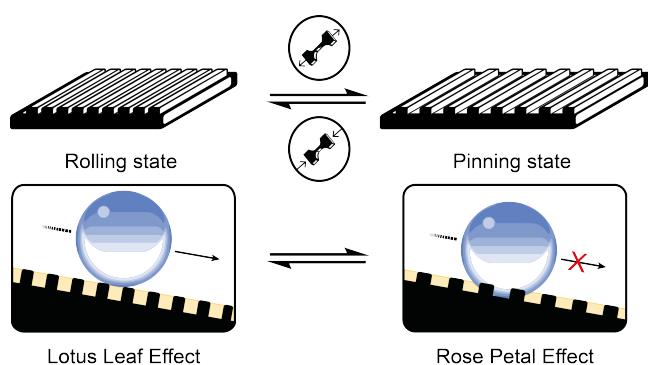


**Figure 7** Mechanoresponsive nanopillar constructs allow for switching between the lotus leaf and rose petal effects owing to capillary forces in the interstitial cavities.<sup>[119]</sup>

show remarkable interactions with water and can be considered as mechanoresponsive materials. Park et al. fabricated black silicon/elastomer composites via a print/transfer process where a PDMS-based elastomer is furnished with small square shaped “Si inks”.<sup>[119]</sup> The stretchable elastomer withstood twelve strain cycles and was able to successfully switch between pinning water droplets and releasing them. In the work of Wang et al., a flexible superhydrophobic PDMS surface was prepared via a direct laser writing process.<sup>[122]</sup> Upon mechanical stretching, the interstitial space between the lamellar nanostructures was widened and, upon relaxation, shortened again. This enabled a reversible switching between lotus leaf and rose petal-like states, where water droplets either are completely repelled from or stuck to the surface. In these initial reports, it was proposed that these smart materials will find applications within the fields of textile and fabric engineering as well as smart surfaces and coatings for biomedical devices or soft robotics.

## Outlook

Nature has long been a source of inspiration for scientists especially for the design and development of materials, in particular those functioning in aqueous environments. Despite researchers’ best efforts, achieving the balance of complexity and functionality that nature exhibits, remains an elusive challenge. Researchers have strived for decades to develop more complex chemical systems that are able to interact in an autonomous and self-regulatory manner, analogous to those found in nature. To achieve this, systems with a high level of both complexity and functionality are required, Figure 8. Beginning with development of organic building blocks and switchable chemical motifs, researchers incorporated these functionalities into systems through the controlled self-assembly and molecular recognition of core structural materials (e.g. polymers, nanoparticles, etc.). Development of hybrid structures and smart polymeric networks were steps towards interactivity. Stimuli-responsive materials surpassed the lower levels of complexity and functionality delivering smart, functional and switchable mate-

rials. Complex interactive materials now represent the next logical level of materials.

As highlighted in this perspective, examples of aqueous interactive materials remain limited. This is despite water being a powerful solvation environment to mediate both intra- and intermolecular self-assembly processes, a requirement for biological adaptive systems. In addition, current systems are mostly restricted to an ON and an OFF state, being able to switch between the two. To be interactive, feedback loops and self-regulatory behavior must be incorporated into these systems. When considering the simplest interactive system, a switch between state A and B (Equation 2), increasing the population of chemical species in state B, for example, should trigger a shift back to state A. In order to switch autonomously, the energy barriers be-

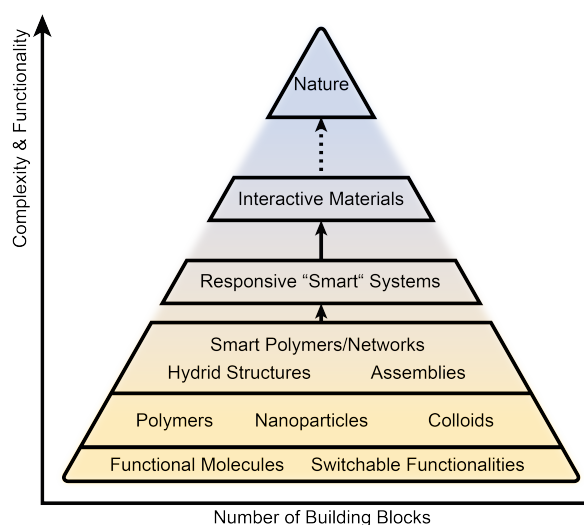


**Figure 8** Roadmap towards interactive materials, ultimately leading to systems with nature-like complexity.

tween states A and B must be lowered. In nature, this is achieved by millions of enzymes, which bring substrates into conformationally-strained positions and lower activation energies to enable chemical transformations. Lower energy barriers between states can help to ensure that interactive systems do not get trapped in a final state lacking any reversibility. Compartmentalization and enhanced control over the timescale of feedback signals, i.e. diffusion of chemical species throughout a system are also important parameters to promote interactive behavior.

Another key pathway towards interactivity should be a focused synthetic effort on the design and synthesis of more sophisticated chemical building blocks that specifically enable lower energy barriers. Yet, this implementation of metastable states should not come at the expense of high conversions between switchable states. Furthermore, chemical moieties should be fully orthogonal and thus act chemo- and regio-selectively at physiological conditions to perform efficiently in an aqueous (biological) environment. Despite their application in the biomedical field, interactive materials

will undoubtedly find wider-reaching applications. The incorporation of logic gates and communication within these materials will expand their utility towards autonomous devices and sensors alongside soft robotics, artificial muscles and energy-harvesting materials.

## Acknowledgements

JAM thanks ESPRC for an IAA KTF. SM is grateful for a Newton International Fellowship. CCP is thankful for the support of an EPSRC PhD Studentship. OAS is thankful to EPSRC Programme Grant NOTCH and ERC Consolidator Grant CAM-RIG.

## References

- [1] J. B. Reece, L. A. Urry, M. L. Cain, S. A. Wasserman, P. V. Minorsky, R. B. Jackson, et al., *Campbell biology*, Pearson Boston, **2014**.
- [2] S. L. Garfinkel, R. H. Grunspan, *The Computer Book: From the Abacus to Artificial Intelligence, 250 Milestones in the History of Computer Science*, Sterling Swift Pub Co, **2018**.
- [3] M. Wei, Y. Gao, X. Li, M. J. Serpe, *Polym. Chem.* **2017**, *8*, 127–143.
- [4] M. W. Urban, *Stimuli-Responsive Materials: From Molecules to Nature Mimicking Materials Design*, Royal Society of Chemistry, **2019**.
- [5] L. Li, J. M. Scheiger, P. A. Levkin, *Advanced Materials* **2019**, *31*, 1807333.
- [6] Y.-J. Kim, Y. T. Matsunaga, *J. Mater. Chem. B* **2017**, *5*, 4307–4321.
- [7] Q. Zhang, C. Weber, U. S. Schubert, R. Hoogenboom, *Mater. Horiz.* **2017**, *4*, 109–116.
- [8] D. Roy, W. L. A. Brooks, B. S. Sumerlin, *Chem. Soc. Rev.* **2013**, *42*, 7214–7243.
- [9] M. Heskins, J. E. Guillet, *J. Macromol. Sci. A* **1968**, *2*, 1441–1455.
- [10] J. Niskanen, H. Tenhu, *Polym. Chem.* **2017**, *8*, 220–232.
- [11] A. C. C. Rotzetter, C. M. Schumacher, S. B. Bubenhofner, R. N. Grass, L. C. Gerber, M. Zeltner, W. J. Stark, *Adv. Mater.* **2012**, *24*, 5352–5356.
- [12] K. Belal, F. Stoffelback, J. Lyskawa, M. Fumagalli, D. Hourdet, A. Marcellan, L. De Smet, V. R. de la Rosa, G. Cooke, R. Hoogenboom, P. Woisel, *Angew. Chem. Int. Ed.* **2016**, *55*, 13974–13978.
- [13] T.-G. La, X. Li, A. Kumar, Y. Fu, S. Yang, H.-J. Chung, *ACS Appl. Mater. Interfaces* **2017**, *9*, 33100–33106.
- [14] Y.-S. Yang, Y. Zhou, F. B. Yin Chiang, Y. Long, *RSC Adv.* **2016**, *6*, 61449–61453.
- [15] C. Nakamura, T. Yamamoto, K. Manabe, T. Nakamura, Y. Einaga, S. Shiratori, *Ind. Eng. Chem. Res.* **2019**, *58*, 6424–6428.
- [16] D. Görl, B. Soberats, S. Herbst, V. Stepanenko, F. Würthner, *Chem. Sci.* **2016**, *7*, 6786–6790.
- [17] T. Hessberger, L. B. Braun, R. Zentel, *Adv. Funct. Mater.* **2018**, *28*, 1800629.
- [18] H. Zhang, A. Mourran, M. Möller, *Nano Lett.* **2017**, *17*, 2010–2014.
- [19] Y. S. Kim, M. Liu, Y. Ishida, Y. Ebina, M. Osada, T. Sasaki, T. Hikima, M. Takata, T. Aida, *Nat. Mater.* **2015**, *14*, 1002.
- [20] H. Xie, J. Shao, Y. Ma, J. Wang, H. Huang, N. Yang, H. Wang, C. Ruan, Y. Luo, Q.-Q. Wang, P. K. Chu, X.-F. Yu, *Biomaterials* **2018**, *164*, 11–21.
- [21] L. Maggini, M. Liu, Y. Ishida, D. Bonifazi, *Adv. Mater.* **2013**, *25*, 2462–2467.
- [22] Y. Shi, H. Ha, A. Al-Sudani, C. J. Ellison, G. Yu, *Adv. Mater.* **2016**, *28*, 7921–7928.
- [23] T. Oehmichen, N. Ise, *Makromol. Chem.* **1991**, *192*, 1107–1114.
- [24] S. Kato, M. Aizawa, S. Suzuki, *J. Membrane Sci.* **1976**, *1*, 289–300.
- [25] M. W. H. Hoorens, W. Szymanski, *Trends Biochem. Sci.* **2018**, *43*, 567–575.
- [26] L. Li, J. M. Scheiger, P. A. Levkin, *Adv. Mater.* **2019**, *31*, 1807333.
- [27] J. M. Christie, J. Gawthorne, G. Young, N. J. Fraser, A. J. Roe, *Mol. Plant* **2012**, *5*, 533–544.
- [28] Y. Zhou, H. Ye, Y. Chen, R. Zhu, L. Yin, *Biomacromolecules* **2018**, *19*, 1840–1857.
- [29] C. S. Linsley, B. M. Wu, *Ther. Deliv.* **2017**, *8*, 89–107.
- [30] O. Bertrand, J.-F. Gohy, *Polym. Chem.* **2017**, *8*, 52–73.
- [31] R. J. Mart, R. D. Osborne, M. M. Stevens, R. V. Ulijn, *Soft Matter* **2006**, *2*, 822.
- [32] F. Ercole, T. P. Davis, R. A. Evans, *Polym. Chem.* **2010**, *1*, 37–54.
- [33] F. A. Jerca, V. V. Jerca, R. Hoogenboom, *Chem* **2017**, *3*, 533–536.
- [34] B. B. Mollet, Y. Nakano, P. C. M. M. Magusin, A. J. H. Spiering, J. A. J. M. Vekemans, P. Y. W. Dankers, E. W. Meijer, *J. Polym. Sci. A* **2016**, *54*, 81–90.
- [35] T. F. Scott, A. D. Schneider, W. D. Cook, C. N. Bowman, *Science* **2005**, *308*, 1615–7.
- [36] G. S. Kumar, D. C. Neckers, *Chem. Rev.* **1989**, *89*, 1915–1925.
- [37] C. Decker, *Prog. Polym. Sci.* **1996**, *21*, 593–650.
- [38] H. Kamogawa, M. Kato, H. Sugiyama, *J. Polym. Sci. A* **1968**, *6*, 2967–2991.
- [39] R. Mogaki, K. Okuro, T. Aida, *J. Am. Chem. Soc.* **2017**, *139*, 10072–10078.
- [40] H. Wang, C. N. Zhu, H. Zeng, X. Ji, T. Xie, X. Yan, Z. L. Wu, F. Huang, *Adv. Mater.* **2019**, *31*, 1807328.
- [41] F. Biedermann, I. Ross, O. A. Scherman, *Polym. Chem.* **2014**, *5*, 5375.
- [42] A. Tabet, R. A. Forster, C. C. Parkins, G. Wu, O. A. Scherman, *Polym. Chem.* **2019**, *10*, 467–472.
- [43] L. Zou, M. J. Webber, *Chem. Commun.* **2019**, *55*, 9931–9934.
- [44] K. A. Günay, T. L. Ceccato, J. S. Silver, K. L. Bannister, O. J. Bednarski, L. A. Leinwand, K. S. Anseth, *Angew. Chem. Int. Ed.* **2019**, *58*, 9912–9916.
- [45] J. Chen, F. K.-C. Leung, M. C. A. Stuart, T. Kajitani, T. Fukushima, E. van der Giessen, B. L. Feringa, *Nat. Chem.* **2018**, *10*, 132–138.
- [46] D. Jaque, L. Martínez Maestro, B. del Rosal, P. Haro-Gonzalez, A. Benayas, J. L. Plaza, E. Martín Rodríguez, J. García Solé, *Nanoscale* **2014**, *6*, 9494–9530.
- [47] X. Huang, S. Neretina, M. A. El-Sayed, *Adv. Mater.* **2009**, *21*, 4880–4910.
- [48] J. S. Basuki, F. Qie, X. Mulet, R. Suryadinata, A. V. Vashi, Y. Y. Peng, L. Li, X. Hao, T. Tan, T. C. Hughes, *Angew. Chem. Int. Ed.* **2017**, *56*, 966–971.
- [49] R. Wang, Z. Yang, J. Luo, I.-M. Hsing, F. Sun, *Proc. Natl. Acad. Sci. U.S.A.* **2017**, *114*, 5912.
- [50] *Electroactive polymer (EAP) actuators as artificial muscles: reality, potential and challenges.* (Ed.: Y. Bar-Cohen), SPIE Press, Bellingham, WA, **2004**.

- [51] L. Romasanta, M. Lopez-Manchado, R. Verdejo, *Prog. Polym. Sci.* **2015**, *51*, 188–211.
- [52] T. Manouras, M. Vamvakaki, *Polym. Chem.* **2017**, *8*, 74–96.
- [53] T. Tanaka, I. Nishio, S.-T. Sun, S. Ueno-Nishio, *Science* **1982**, *218*, 467–469.
- [54] D. Morales, E. Palleau, M. D. Dickey, O. D. Velev, *Soft Matter* **2014**, *10*, 1337–1348.
- [55] C. Yang, W. Wang, C. Yao, R. Xie, X.-J. Ju, Z. Liu, L.-Y. Chu, *Sci. Rep.* **2015**, *5*, 13622.
- [56] C. Yang, Z. Liu, C. Chen, K. Shi, L. Zhang, X.-J. Ju, W. Wang, R. Xie, L.-Y. Chu, *ACS Appl. Mater. Interfaces* **2017**, *9*, 15758–15767.
- [57] H. Jiang, L. Fan, S. Yan, F. Li, H. Li, J. Tang, *Nanoscale* **2019**, *11*, 2231–2237.
- [58] N. Ozaki, H. Sakamoto, T. Nishihara, T. Fujimori, Y. Hijikata, R. Kimura, S. Irlle, K. Itami, *Angew. Chem. Int. Ed.* **2019**, *56*, 11196–11202.
- [59] A. Omidinia-Anarkoli, S. Boesveld, U. Tuvshindorj, J. C. Rose, T. Haraszti, L. De Laporte, *Small* **2017**, *13*, 1702207.
- [60] J. C. Rose, M. Cámara-Torres, K. Rahimi, J. Köhler, M. Möller, L. De Laporte, *Nano Lett.* **2017**, *17*, 3782–3791.
- [61] Y. D. Liu, H. J. Choi, *Soft Matter* **2012**, *8*, 11961–11978.
- [62] Y. Z. Dong, Y. Seo, H. J. Choi, *Soft Matter* **2019**, *15*, 3473–3486.
- [63] G. Hernández-Vargas, C. A.P.-P. de León, J. González-Valdez, H. M. N. Iqbal, *Sep. Purif. Rev.* **2018**, *47*, 199–213.
- [64] X. Hou, Y. Liu, G. Wan, Z. Xu, C. Wen, H. Yu, J. X. J. Zhang, J. Li, Z. Chen, *Appl. Phys. Lett.* **2018**, *113*, 221902.
- [65] A. A. Adedoyin, A. K. Ekenseair, *Nano Res.* **2018**, *11*, 5049–5064.
- [66] D. Szabó, G. Szeghy, M. Zrínyi, *Macromolecules* **1998**, *31*, 6541–6548.
- [67] J. Thévenot, H. Oliveira, O. Sandre, S. Lecommandoux, *Chem. Soc. Rev.* **2013**, *42*, 7099–7116.
- [68] T. Blin, A. Niederberger, L. Benyahia, J. Fresnais, V. Montebault, L. Fontaine, *Polym. Chem.* **2018**, *9*, 4642–4650.
- [69] M. Zrínyi, L. Barsi, A. Büki, *J. Chem. Phys.* **1996**, *104*, 8750–8756.
- [70] A. P. Safronov, E. A. Mikhnevich, Z. Lotfollahi, F. A. Blyakhman, T. F. Sklyar, A. Larrañaga Varga, A. I. Medvedev, S. Fernández Armas, G. V. Kuryandskaya, *Sensors* **2018**, *18*.
- [71] S. Herrera-Posada, C. Mora-Navarro, P. Ortiz-Bermudez, M. Torres-Lugo, K. M. McElhinny, P. G. Evans, B. O. Calcagno, A. Acevedo, *Mater. Sci. Eng. C* **2016**, *65*, 369–378.
- [72] Y. Cao, M. Hassan, Y. Cheng, Z. Chen, M. Wang, X. Zhang, Z. Haider, G. Zhao, *ACS Appl. Mater. Interfaces* **2019**, *11*, 12379–12388.
- [73] C. Pitakchatwong, S. Chirachanchai, *ACS Appl. Mater. Interfaces* **2017**, *9*, 10398–10407.
- [74] M. Helminger, B. Wu, T. Kollmann, D. Benke, D. Schwahn, V. Pipich, D. Faivre, D. Zahn, H. Cölfen, *Adv. Funct. Mater.* **2014**, *24*, 3187–3196.
- [75] E. I. Wisotzki, D. Eberbeck, H. Kratz, S. G. Mayr, *Soft Matter* **2016**, *12*, 3908–3918.
- [76] T. Nypelö, C. Rodriguez-Abreu, J. Rivas, M. D. Dickey, O. J. Rojas, *Cellulose* **2014**, *21*, 2557–2566.
- [77] P. Dhar, A. Kumar, V. Katiyar, *ACS Appl. Mater. Interfaces* **2016**, *8*, 18393–18409.
- [78] R. Weeber, M. Hermes, A. M. Schmidt, C. Holm, *J. Phys. Condens. Matter* **2018**, *30*, 063002.
- [79] P. Papaphilippou, M. Christodoulou, O.-M. Marinica, A. Taculescu, L. Vekas, K. Chrissafis, T. Krasia-Christoforou, *ACS Appl. Mater. Interfaces* **2012**, *4*, 2139–2147.
- [80] J. Qin, I. Asempah, S. Laurent, A. Fornara, R. N. Muller, M. Muhammed, *Adv. Mater.* **2009**, *21*, 1354–1357.
- [81] S. Reinicke, S. Döhler, S. Tea, M. Krekhova, R. Messing, A. M. Schmidt, H. Schmalz, *Soft Matter* **2010**, *6*, 2760–2773.
- [82] X. Lin, B. Nguyen Quoc, M. Ulbricht, *ACS Appl. Mater. Interfaces* **2016**, *8*, 29001–29014.
- [83] B. A. Badeau, M. P. Comerford, C. K. Arakawa, J. A. Shadish, C. A. DeForest, *Nat. Chem.* **2018**, *10*, 251–258.
- [84] A. Shastri, L. M. McGregor, Y. Liu, V. Harris, H. Nan, M. Mujica, Y. Vasquez, A. Bhattacharya, Y. Ma, M. Aizenberg, O. Kuksenok, A. C. Balazs, J. Aizenberg, X. He, *Nat. Chem.* **2015**, *7*, 447–454.
- [85] H. Cui, Q. Zhao, Y. Wang, X. Du, *Chem. Asian J.* **2019**, *14*, 2369–2387.
- [86] H. Lu, W. Huang, *Chemo-responsive shape-memory polymers for biomedical applications*, Woodhead Publishing, **2015**, pp. 99–132.
- [87] V. V. Yashin, O. Kuksenok, P. Dayal, A. C. Balazs, *Rep. Prog. Phys.* **2012**, *75*, 066601.
- [88] D. Roy, J. N. Cambre, B. S. Sumerlin, *Prog. Polym. Sci.* **2010**, *35*, 278–301.
- [89] N. Eloom Dov, S. Shankar, D. Cohen, T. Bendikov, K. Rechav, L. J. W. Shimon, M. Lahav, M. E. van der Boom, *J. Am. Chem. Soc.* **2017**, *139*, 11471–11481.
- [90] M. V. Sussman, A. Katchalsky, *Science* **1970**, *167*, 45–7.
- [91] M. Nakahata, Y. Takashima, H. Yamaguchi, A. Harada, *Nat. Commun.* **2011**, *2*, 511.
- [92] M. Nakahata, Y. Takashima, A. Hashidzume, A. Harada, *Angew. Chem. Int. Ed.* **2013**, *52*, 5731–5735.
- [93] A. S. Carlini, R. Gaetani, R. L. Braden, C. Luo, K. L. Christman, N. C. Gianneschi, *Nat. Commun.* **2019**, *10*, 1735.
- [94] M. P. Lutolf, J. L. Lauer-Fields, H. G. Schmoekel, A. T. Metters, F. E. Weber, G. B. Fields, J. A. Hubbell, *Proc. Natl. Acad. Sci. U.S.A.* **2003**, *100*, 5413–8.
- [95] N. Joshi, J. Yan, S. Levy, S. Bhagchandani, K. V. Slaughter, N. E. Sherman, J. Amirault, Y. Wang, L. Riegel, X. He, T. S. Rui, M. Valic, P. K. Vemula, O. R. Miranda, O. Levy, E. M. Gravallese, A. O. Aliprantis, J. Ermann, J. M. Karp, *Nat. Commun.* **2018**, *9*, 1275.
- [96] D. E. Clarke, C. D. J. Parmenter, O. A. Scherman, *Angew. Chem. Int. Ed.* **2018**, *57*, 7709–7713.
- [97] D. Spitzer, L. L. Rodrigues, D. Straßburger, M. Mezger, P. Besenius, *Angew. Chem. Int. Ed.* **2017**, *56*, 15461–15465.
- [98] Y. Hisamatsu, S. Banerjee, M. B. Avinash, T. Govindaraju, C. Schmuck, *Angew. Chem. Int. Ed.* **2013**, *52*, 12550–12554.
- [99] M. Externbrink, S. Riebe, C. Schmuck, J. Voskuhl, *Soft Matter* **2018**, *14*, 6166–6170.
- [100] X. He, M. Aizenberg, O. Kuksenok, L. D. Zarzar, A. Shastri, A. C. Balazs, J. Aizenberg, *Nature* **2012**, *487*, 214–218.
- [101] C. R. Hickenboth, J. S. Moore, S. R. White, N. R. Sottos, J. Baudry, S. R. Wilson, *Nature* **2007**, *446*, 423 EP –.
- [102] H. Chen, F. Yang, Q. Chen, J. Zheng, *Adv. Mater.* **2017**, *29*, 1606900.
- [103] Y. Sagara, M. Karman, A. Seki, M. Pannipara, N. Tamaoki, C. Weder, *ACS Cent. Sci.* **2019**, *5*, 874–881.
- [104] T. Matsuda, R. Kawakami, R. Namba, T. Nakajima, J. P. Gong, *Science* **2019**, *363*, 504–508.
- [105] R. Merindol, G. Delechiave, L. Heinen, L. H. Catalani, A. Walther, *Nat. Commun.* **2019**, *10*, 528.
- [106] B. Xin, J. Hao, *Chem. Soc. Rev.* **2010**, *39*, 769–782.
- [107] S. Wang, L. Jiang, *Adv. Mater.* **2007**, *19*, 3423–3424.

- [108] N. J. Shirtcliffe, G. McHale, S. Atherton, M. I. Newton, *Adv. Colloid Interface Sci.* **2010**, *161*, 124–138.
- [109] B. Wang, W. Liang, Z. Guo, W. Liu, *Chem. Soc. Rev.* **2015**, *44*, 336–361.
- [110] F. Guo, Z. Guo, *RSC Adv.* **2016**, *6*, 36623–36641.
- [111] V. A. Ganesh, A. S. Ranganath, R. Sridhar, H. K. Raut, S. Jayaraman, R. Sahay, S. Ramakrishna, A. Baji, *Macromol. Rapid Commun.* **2015**, *36*, 1368–1373.
- [112] W. Zhang, N. Liu, Q. Zhang, R. Qu, Y. Liu, X. Li, Y. Wei, L. Feng, L. Jiang, *Angew. Chem. Int. Ed.* **2018**, *57*, 5740–5745.
- [113] J.-J. Li, Y.-N. Zhou, Z.-H. Luo, *ACS Appl. Mater. Interfaces* **2015**, *7*, 19643–19650.
- [114] H. Gao, Y. Liu, S. Li, G. Wang, Z. Han, L. Ren, *Nanoscale* **2018**, *10*, 15393–15401.
- [115] J. Zhang, J. Yong, Q. Yang, F. Chen, X. Hou, *Langmuir* **2019**, *35*, 3295–3301.
- [116] L. Lei, Q. Zhang, S. Shi, S. Zhu, *Langmuir* **2017**, *33*, 11936–11944.
- [117] C. Zong, M. Hu, U. Azhar, X. Chen, Y. Zhang, S. Zhang, C. Lu, *ACS Appl. Mater. Interfaces* **2019**, *11*, 25436–25444.
- [118] E. Cohen, Y. Soffer, H. Weissman, T. Bendikov, Y. Schilt, U. Raviv, B. Rybtchinski, *Angew. Chem. Int. Ed.* **2018**, *57*, 8871–8874.
- [119] J. K. Park, Z. Yang, S. Kim, *ACS Appl. Mater. Interfaces* **2017**, *9*, 33333–33340.
- [120] D.-M. Drotlef, P. Blümler, P. Papadopoulos, A. del Campo, *ACS Appl. Mater. Interfaces* **2014**, *6*, 8702–8707.
- [121] C. Chen, Z. Huang, Y. Jiao, L.-A. Shi, Y. Zhang, J. Li, C. Li, X. Lv, S. Wu, Y. Hu, W. Zhu, D. Wu, J. Chu, L. Jiang, *ACS Nano* **2019**, *13*, 5742–5752.
- [122] J.-N. Wang, Y.-Q. Liu, Y.-L. Zhang, J. Feng, H. Wang, Y.-H. Yu, H.-B. Sun, *Adv. Funct. Mater.* **2018**, *28*, 1800625.